Impact of deoxygenation and hydrological changes on the Black Sea nitrogen cycle during the Last Deglaciation and Holocene

Anna Cutmore[1*]., Nicole Bale[1]., Rick Hennekam[2]., Bingjie Yang[1]., Darci Rush[1]., Gert-Jan Reichart[2,3]., Ellen C. Hopmans[2]., Stefan Schouten[1,3]

[1]*Department of Marine Microbiology & Biogeochemistry, NIOZ Royal Netherlands Institute for Sea Research, 1790 AB Den Burg, Netherlands*

[2]*Department of Ocean Systems, NIOZ Royal Netherlands Institute for Sea Research, 1790 AB Den Burg, Netherlands*

[3]*Department of Earth Sciences, Universiteit Utrecht, Princetonlaan 8a, 3584 CB Utrecht, Netherlands*

*Corresponding Author: anna.cutmore@nioz.nl

Abstract

The marine nitrogen (N) cycle profoundly impacts global ocean productivity. Amid rising deoxygenation in marine environments due to anthropogenic pressures, understanding the impact of this on the marine N-cycle is vital. The Black Sea's evolution from an oxygenated lacustrine basin to an anoxic marine environment over the last deglaciation and Holocene offers insight into these dynamics. Here, we generated records of the organic biomarkers heterocyte glycolipids, crenarchaeol, and bacteriohopanetetrol, associated with various water-column microbial N-cycle processes, which indicate a profound change in Black Sea N-cycle dynamics at ~7.2 ka when waters became severely deoxygenated. This transition substantially reduced Thaumarchaeota-driven nitrification and enhanced loss of bioavailable nitrogen through anaerobic ammonium oxidation (anammox)~~anammox~~. In contrast, other climatic changes over the last deglaciation and Holocene, such as freshwater input, water-level variations and temperature changes, did not impact these processes. Cyanobacterial nitrogen fixation in surface waters proved more responsive to changes in salinity which affected species composition, ~~-~~and associated water column stratification which reduced vertical transport of nutrients. Our results indicate that future deoxygenation in certain ~~–~~marine environments may enhance bioavailable nitrogen loss by anammox and reduce nitrification by Thaumarchaeota, while enhanced stratification may increase cyanobacterial nitrogen fixation in the surface waters.

1. Introduction

The marine nitrogen (N) cycle is a significant control of biological productivity in ~~our~~ the global oceans. It is directly connected to the fixation of atmospheric carbon dioxide and carbon export from the ocean's surface, influencing atmospheric CO_2 levels over geological time scales (Falkowski et al., 1998). As the marine N-cycle is strongly regulated by biology, the (de)oxygenation of the ocean determines the microorganisms involved in these biogeochemical cycles and the aerobic/anaerobic pathways that occur. Under anoxic conditions, loss of bioavailable nitrogen is substantial, attributed to anaerobic ammonium oxidation (anammox) and denitrification (Kuypers et al., 2003; Dalsgaard et al., 2012). With deoxygenation in marine environments increasing due to anthropogenic climate and environmental changes (i.e., Keeling et al., 2010; Bopp et al., 2013), and research linking deoxygenation to changes in the marine N-cycle (Kalvelage et al., 2013; Naafs et al., 2019), it is important

to enhance our understanding of how the marine N-cycle may respond to future deoxygenation and what the associated feedbacks on carbon fixation might be.

Marine basins that have experienced changes in oxygenation in the past can provide perspective on the current deoxygenation of modern global oceans and the associated feedbacks in the marine N-cycle, in particular on timescales beyond the observational record. Today, the Black Sea is the world's largest permanently stratified anoxic basin with limited connection to the global ocean through the Bosporus Strait and its redox gradient is a hotspot of diverse microbial populations and metabolisms, experiencing many of the same crucial microbial biogeochemical cycle processes as the global ocean (Kusch et al., 2022). However, over the last deglaciation and Holocene (approximately the last 20 ka), the Black Sea experienced large hydrological changes. The basin was an oxygenated fresh-water lacustrine environment during the Last Glacial Maximum (LGM) (Schrader, 1979) and experienced many environmental changes during the subsequent deglaciation, including temperature changes (Bahr et al., 2005; 2008; Ion et al., 2022), water-level variations (Ivanova et al., 2007; Nicholas et al., 2011; Piper & Calvert, 2011), and changes in freshwater input into the basin, both through melting of Eurasian icesheets and alpine glaciers after the LGM and changes in regional precipitation (Bahr et al., 2005; 2006; 2008; Badertscher et al., 2011; Shumilovskikh et al., 2012). It became reconnected to the global ocean at ~9.6 ka when post-glacial sea-level rise caused an initial marine inflow (IMI) over the Bosporus sill (Aksu et al., 2002; Major et al., 2006; Bahr et al., 2008; Ankindinova et al., 2019), leading to enhanced salinity of the water column (Marret et al., 2009; Verleye et al., 2009; Filipova-Marinova et al., 2013) and euxinic deep waters developing in the basin after ~7.2 ka (Arthur & Dean, 1998; Eckert et al., 2013). Thus, sedimentary records of the Black Sea may provide a unique perspective of the impact of deoxygenation, as well as changing temperature and salinity, on the marine N-cycle.

Diagnostic lipid biomarkers of microbes preserved in the geological record can offer a unique insight into past changes in the N-cycle (Rush & Sinninghe Damsté, 2017 and references cited therein; Elling et al., 2021; van Kemenade et al., 2023), although the limitations of extrapolating modern findings to ancient climates must be acknowledged, as past ecosystems may have operated under different dynamics that are not fully captured by contemporary analogues. Nitrogen fixing heterocytous cyanobacteria play a crucial role in transforming nitrogen gas (N_2) to bioavailable nitrogen (NH_3) and sustaining primary productivity in both marine and freshwater environments (Villareal, 1992; Ploug et al., 2008). Identification of their diagnostic biomarkers, heterocyte glycolipids (HGs), in the geological record are a widely-used proxy for ~~enables~~ explor~~ingation of~~ past changes in nitrogen fixation by these microbes (Bauersachs et al., 2009; 2010; Sollai et al., 2017; Bale et al., 2019; Elling et al., 2021; Pérez Gallego et al., 2025). The structure of the sugar moiety of HGs is a useful indicator of paleoenvironmental conditions, as HGs with a hexose (C_6) headgroup are typically found in free-living heterocystous cyanobacteria (Bauersachs et al, 2009; Wörmer et al., 2012), while HGs with a pentose (C_5) headgroup are associated with endosymbiotic heterocystous cyanobacteria in marine diatoms (diatom-diazotroph associations, DDAs) (Schouten et al., 2013; Bale et al., 2015). Consequently, both hexose and pentose HGs have been applied as specific paleo-biomarkers for the presence of N_2-fixing cyanobacteria in marine and

lacustrine geological records (Bauersachs et al., 2010; Sollai et al., 2017; Bale et al., 2019; Elling et al., 2021). Nitrification, the microbial two-step conversion of ammonia (NH_3) and/or ammonium (NH_4^+) to nitrate (NO_3-), is a central part of the marine N-cycle. Archaea of the phylum Thaumarchaeota (also known as Nitrososphaerota) are among the most abundant and widespread marine prokaryotes (Karner et al., 2001; Francis et al., 2005), playing a crucial role in nitrification in the Black Sea (Lam et al., 2007) by aerobically oxidizing ammonia to nitrite (Könneke et al., 2005; Wuchter et al., 2006). As Thaumarchaeota are the exclusive producers of the membrane spanning lipid, crenarchaeol (Sinninghe Damste et al., 2002), this biomarker can be used to identify Thaumarchaeota in the geological record and explore the palaeo marine N-cycle. Another critical part of the N-cycle is the loss of bioavailable nitrogen to N_2. Under anoxic conditions, bioavailable nitrogen (NO_3-, NO_3-, NH_3 and NH_4^+) can be lost through two processes in subsurface waters: anammox (van de Graaf et al., 1997; Kuypers et al., 2003) and denitrification (Kuenen and Robertson, 1988). It is possible to explore past changes in anammox activity in the sedimentary record using the unique ladderane fatty acids (Sinninghe Damste et al., 2002) but these are relatively poorly preserved in sediments (Jaeschke et al., 2007). Alternatively, the ratio of bacteriohopanetetrol (BHT)-34S (which is ubiquitously synthesized by aerobic bacteria) and the later eluting stereoisomer BHT-x (which is predominately synthesized by marine anammox bacteria, i.e., Ca. Scalindua spp.) (Rush et al., 2014; Schwartz-Narbonne et al., 2020; van Kemenade et al., 2023) can be used to trace past anammox activity. Denitrification is performed by a large range of organisms (Knowles, 1982), but at present, there are no associated diagnostic lipid biomarkers (Rush et al., 2017).

In this study, we used lipid biomarkers of microbes widely involved in the N-cycle across various marine and freshwater environments in combination with other geochemical records from a sediment core located in the western Black Sea spanning the last deglaciation and Holocene (~20 ka – present) to better constrain and assess the sensitivity of the marine N-cycle under changing hydrological and oxygenation conditions and explore its potential links to broader global climate dynamics.

2. Regional Setting

The Black Sea is a large meromictic marginal basin connected to the Mediterranean Sea via the Turkish Straits (the Bosporus, the Sea of Marmara, and the Dardanelles Strait) (Fig. 1). The Black Sea has a net outflow into the Aegean Sea via the Turkish Straits, and is primarily supplied by three major rivers, the Danube, Dnieper, and Don. With freshwater flowing out of the basin and dense, highly saline waters flowing in, the water column is highly stratified with respect to salinity (density). An oxygenated colder surface layer (0 – 50 m) overlies warmer, anoxic, sulfidic, hypersaline deep waters (100 – 2300 m), separated by a suboxic layer (50 – 100 m) (Murray et al., 1989; 1995). The general circulation of Black Sea surface-waters is a basin-scale cyclonic boundary current encompassing large eastern and western cyclonic gyres, with several smaller, anticyclonic coastal eddies (Fig. 1) (Özsoy and Ünlüata, 1997). The modern Black Sea water column is characterized by the presence of strong redox gradients. In the basin's western gyre, the oxic zone (0 – 75 m depth range) has an oxygen concentration of ~121 µmol/kg and salinity of 19.4 psu at 50 m depth, with no detectable sulfide concentrations (Sollai et al., 2018; Bale et al., 2021). The suboxic zone lies below (75 – 115 m depth range), where salinity increases with depth and

traces of sulfide are detected at the bottom of this layer at ~110 m (Sollai et al., 2018; Bale et al., 2021). Beneath this lies the euxinic zone (115 – 2000 m depth range), where salinity and sulfide concentrations increase with depth, reaching 22.3 psu and ~400 µmol/L at a depth of 2,000 m (Sollai et al., 2018; Bale et al., 2021). Ammonium concentrations are low in the oxic and upper suboxic zones (<0.1 µmol/L), increasing below 90 m, with highest concentrations (~100 µmol/L) at 2000 m water depth (Sollai et al., 2018). Nitrite concentrations are highest in the oxic zone, peaking at 50 m (~0.08 µmol/L), decreasing through the suboxic zone, with the exception of a peak at 85 m, while in the euxinic zone, nitrite is below the limit of detection (Sollai et al., 2018). Nitrate concentrations are highest in the lower oxic and upper suboxic zones, peaking between 70 – 80 m (~2.5 µmol/L), decreasing with depth and reaching the limit of detection below 105 m (Sollai et al., 2018; Bale et al., 2021).

3. Methods

During the cruise with the RV Pelagia in April 2017, piston core 64PE418 (235 cm length) was recovered from 1970 m below sea level (mbsl) depth in the Black Sea (42°56 N, 30°02 E) (Fig. 1). 44 sediment samples were taken at 5 cm intervals along the depth of the core.

3.1. Biomarker extraction and analysis

Lipids were extracted from these samples using a modified Bligh and Dyer extraction method as described previously (Bale et al., 2021). Using a mixture of methanol (MeOH), dichloromethane (DCM), and phosphate buffer (2:1:0.8, v:v), the sediment was twice extracted ultrasonically (10 min). The combined supernatants were phase-separated by adding DCM and phosphate buffer to create a solvent ratio of 1:1:0.9 (v:v). The organic phase was collected, and the aqueous phase re-extracted three times using DCM. All extraction steps were then repeated on the residue but with a mixture of MeOH, DCM and aqueous trichloroacetic acid solution (TCA) pH 3 (2:1:0.8, v:v). Finally, the organic extracts were combined and dried under a N_2 gas stream. A deuterated betaine lipid {1,2-dipalmitoyl-sn-glycero-3-O-4'-[N,N,N-trimethyl(d9)]-homoserine; Avanti Lipids} internal standard was added to each sample before filtering the extract through 0.45 µm cellulose syringe filters (4 mm diameter; BGB, USA). Extraction blanks were performed alongside the sediment extractions, using the same glassware, solvents and extraction methodology, but without sediment. Analysis of the extracts was performed using the following UHPLC-HRMS reversed phase method. An Agilent 1290 Infinity I UHPLC was used, equipped with thermostatted auto-injector and column oven, coupled to a Q Exactive Orbitrap MS with Ion Max source ~~with~~ using heated electrospray ionization (HESI) probe (Thermo Fisher Scientific, Waltham, MA). Separation was achieved using an Acquity BEH C18 column (Waters, 2.1 × 150 mm, 1.7 µm) maintained at 30°C. The eluent composition was (A) MeOH/H_2O/formic acid/14.8 M NH_3aq [85:15:0.12:0.04 (v:v)] and (B) IPA/MeOH/formic acid/14.8 M NH_3aq [50:50:0.12:0.04 (v:v)]. The elution program was: 95% A (for 3 min) followed by a linear gradient to 40% A (at 12 min) and then to 0% A (at 50 min), which was maintained until 80 min. The flow rate was 0.2 mL min^{-1}. Positive ion HESI settings were: capillary temperature, 300°C; sheath gas (N_2) pressure, 40 arbitrary units (AU); auxiliary gas (N_2) pressure, 10 AU; spray voltage, 4.5 kV; probe heater temperature, 50°C; S-lens 70 V. Lipids were analyzed with a mass range of *m/z* 350–2000 (resolving power 70,000 ppm at *m/z* 200), followed by data-dependent tandem MS/MS (resolving power 17,500 ppm), in which the 10 most abundant

masses in the mass spectrum were fragmented successively. Optimal fragmentation was achieved with a stepped normalized collision energy of 15, 22.5 and 30 (isolation width, 1.0 *m/z*) for IPL analysis (Bale et al., 2021) and 22.5 and 40 (isolation width 1.0 *m/z*) for BHP analysis (Hopmans et al., 2021). The Q Exactive was calibrated within a mass accuracy range of 1 ppm using the Thermo Scientific Pierce LTQ Velos ESI Positive Ion Calibration Solution. During analysis, dynamic exclusion was used to temporarily exclude masses (for 6 s) to allow selection of less abundant ions for MS/MS.

Biomarkers were identified based on their retention time, exact mass, and fragmentation spectra. Integrations were performed on (summed) mass chromatograms of relevant molecular ions ($[M+H]^+$, $[M+NH4]^+$, and $[M+Na]^+$) and in the case of crenarchaeol also the second isotope peak for each of the three adducts. Due to coelution of BHT-34S, BHT-x isomer and an unknown nitrogen containing compound with the same mass, identification and integration of BHT-34S and BHT-x was conducted using the *m/z* 529.462 dehydrated insource product ($[M+H]^+$-H_2O). Isoprenoidal glycerol dialkyl glycerol tetraether (isoGDGT) crenarchaeol, monohexose crenarchaeol, and a crenarchaeol isomer were all integrated and combined as 'crenarchaeol'. The lipid biomarker records are all presented as peak area per gram of total organic carbon (TOC).

3.2. Total organic carbon and total nitrogen and $\delta^{15}N_{bulk}$ measurements

Freeze-dried sediments were analysed for TOC, total nitrogen (TN) and bulk $\delta^{15}N$ ($\delta^{15}N_{bulk}$) using a ThermoScientific Flash EA Delta V Plus IRMS. Flow was 100 ml/min and the temperature for oxidation, reduction and the oven were 900°C, 680°C, and 40°C, respectively. Nitrogen isotopic measurements were calibrated to atmospheric air (AIR) and values are expressed in permil (‰) units. Inorganic carbon was removed from the sediment prior to TOC analysis using HCl (2 mol), cleaned with bi-distilled water, then freeze-dried.

3.3. Age model

Accelerator Mass Spectrometry (AMS) ^{14}C ages of bulk organic matter were measured from core 64PE418 (n = 7) to create a chronology on the 64PE418 depth scale. Samples were weighed and freeze-dried at NIOZ. The AMS ^{14}C measurements ($^{14}C/\ ^{12}C$) were determined using a Compact Carbon AMS System at the Poznań Radiocarbon Laboratory, Poland. The sediment samples were pre-treated with 0.25M HCl (room temperature overnight, then 80°C, 1+ hour), and rinsed with deionised water until pH = 7. Samples were then combusted in closed (sealed under vacuum) quartz tubes, together with CuO and Ag wool (900°C, 10 hours). The CO_2 released was then dried in a vacuum line and reduced with H_2 using 2 mg of iron (Fe) powder as a catalyst. The obtained carbon and Fe mixture was then pressed into an aluminium holder (Czernik & Goslar, 2001). The measurement was performed by comparing intensities of ionic beams of ^{14}C, ^{13}C and ^{12}C measured for each sample and for standard samples (with "Oxalic Acid II" used as modern standard; "coal" used as background standard of ^{14}C-free carbon). In each AMS run, 30-33 samples of unknown age were measured, alternated with measurements of 3-4 samples of modern standard and 1-2 samples of background standard. The measured $^{14}C/\ ^{12}C$ ratios are corrected for isotopic fractionation and reported as conventional radiocarbon age according to Stuiver & Polach (1977).

Seven bulk organic matter ^{14}C dates were used in the production of the age-model for core 64PE418 (Table S1 and Fig. S1). Six of these were from this core, with an additional bulk organic carbon ^{14}C date from the widely acknowledged Unit I/II boundary of core KNR 134-08 BC17, which was used to further refine the age model for the upper part of the core (Jones & Gagnon, 1994). Core KNR 134-08 BC17 was sourced from the same location and water depth as 64PE418 and this boundary was identified in our core using the same significant colour and elemental changes described in previous studies (Fig. 2 and 3) (i.e., Arthur & Dean, 1998; Bahr et al., 2005). While seven ^{14}C measurements were conducted on core 64PE418, one was excluded from the age model due to an age reversal (142.5 cm), likely due to the presence of reworked material, which would have made the age model out of line with other studies (Fig. S2). Variable reservoir-ages were added to our calibration (Table S1), using those calculated by Kwiecien et al., (2008) for intermediate water depths in the Black Sea over the last deglaciation and Holocene which were deemed the most suitable for our site location. The ^{14}C dates were calibrated using the Marine20 calibration curve (Heaton et al., 2020) for the upper three samples (24.5, 39, 76.5 cm) which reflect the period after the infiltration of marine water; this is based on the colour and elemental changes in the core which indicate that these samples fall within Units I and II (Arthur & Dean, 1998; Bahr et al., 2005). The lower four samples (118.5, 158.5, 183.5 and 217.5 cm) were calibrated using the IntCal20 calibration curve (Reimer et al., 2020), as they reflect the period prior to the marine infiltration when then Black Sea was a lacustrine environment, as indicated by colour and elemental signatures in the core (Arthur & Dean, 1998; Bahr et al., 2005). Using the R-code CLAM (Blaauw, 2010), the age–depth model was created based on the seven ^{14}C dates. Our age model shows that the 64PE418 biomarker records span the last 19.5 ka, with an average resolution of ~450 years. The following transitions are identified in our core by colour (Fig. 2S1) and elemental changes (Fig. 3S2) and dated by our age model as follows: the onset of the IMI (138 cm) is at 9.6 ka ± 237 yrs, the boundary of Unit II/III (96 cm) is dated at 7.2 ka ± 202 yrs, and the Unit I/II boundary (39 cm) is dated at 2.6 ka ± 402 yrs. The Despite the complexity of dating Black Sea cores, due to lack of suitable material for dating and dispute over reservoir age corrections (Kwecien et al., 2008; Soulet et al., 2011; Yanchilina et al. 2017), the dates of these boundaries align well with previously published calibrated ages for these transitions (i.e., Jones & Gagnon, 1994; Ankindinova et al., 2019; Huang et al., 2021), as shown in Fig. S2.

4. Results

4.1. TOC, TN and colour changes

Sedimentary bulk TOC (%), bulk TN (%), and $\delta^{15}N_{bulk}$ (‰) range between 0.3 – 22.8% for TOC and 0.05 – 1.9% for TN, and 5.2 – 0.0‰ for $\delta^{15}N_{bulk}$ (Fig. 4). There are significant colour changes in the core, as shown in Fig. 2S1 which correspond to changes in TOC, TN and the elemental composition (Fig. 3. S2). In the lower part of the core (19.5 – 9.6 ka), values are relatively low for TOC and TN, at ~0.84% and ~0.10%, respectively. At 9.6 ka, there is an appreciable change in the elemental composition of the core, with increases in Ti/Ca, K and V and a decrease in Mn/Al, which corresponds with a transition to darker sediments and an increase in TOC and TN to ~2.41% and ~0.26%, respectively. At 7.2 ka there is another major change in the colour and bulk elemental composition of

the core, with an increase in redox-sensitive elements U, V, and Mo and a decrease in Ti/Ca and K (Fig. 3~~, S2~~), which corresponds with darker sediments and increasing TOC values. TOC peaks between 6.6 – 4.6 ka (~21% for TOC and ~1.7% for TN), declining towards the top of the core. $\delta^{15}N_{bulk}$ shows a general decline in values from the upper to the lower part of the core. This decline is small between 19.5 – 7.7 ka (4.9 – 3.3‰), before a more significant decrease to 1.2‰ at 6.6 ka (3.3 – 1.2‰). Values increase to 3.7‰ at 6.1 ka before declining to 0.0‰ at 3.9 ka, increasing slightly towards the top of the core to values of 1.3‰.

4.2. Biomarkers

We examined a number of lipid biomarkers related to the N-cycle in Black Sea core 64PE418 (Fig. 4). HGs were identified in all samples (with the exception of 215 cm (16.4 ka)). These include HGs with a hexose (C_6) headgroup i.e., hexose C_{26} diol, hexose C_{28} diol, hexose C_{28} triol and hexose C_{30} triol, which are specific to free-living cyanobacteria, found in predominately freshwater and brackish environments (Bauersachs et al, 2009; Wörmer et al., 2012). In addition, those with a pentose (C_5) headgroup i.e., pentose C_{30} diol, pentose C_{30} triol, pentose C_{32} triol were detected which are specific to cyanobacteria symbiotic with marine ~~-~~diatoms ~~(diatom-diazotroph associations, DDAs)~~ (Schouten et al., 2013; Bale et al., 2015). Hexose HGs are present throughout the core, increasing substantially in abundance between 9.6 – 6.6 ka, reaching maximum values at 9.6 ka. Pentose HGs are detected from 4.3 ka onwards, increasing in abundance at the top of the record coinciding with low abundance of hexose HGs. Crenarchaeol, a marker for Thaumarchaeota, was identified throughout our record, showing high values in the early part of the record (~ 1.1E+14 peak area per g TOC) until 6.9 ka, abruptly shifting to lower values ~ 3.9E+13 peak area per g TOC thereafter. The BHT-x ratio, a biomarker for anammox bacteria, is low in the early part of our record (<0.3), due to low abundance of BHT-x. The BHT-x ratio increases after 6.9 ka to values around 0.3, due to higher abundance of BHT-x and lower abundance of BHT with a 34S stereoconfiguration.

Finally, to reconstruct levels of oxygen in the subsurface waters of the Black Sea, isorenieratene was identified (as described in Bale et al., 2021). Isorenieratene is a marker of the brown-coloured strains of the photosynthetic green sulfur bacteria, Chlorobiaceae, which are anoxygenic photoautotrophs that require light and hydrogen sulphide (H_2S); their presence indicates photic zone euxinia, whereby anoxic, sulfidic waters reached the photic zone (Sinninghe Damste et al., 1993; Koopmans et al., 1996). Isorenieratene was identified in many of our samples after 9.5 ka, peaking between 5.6 – 4.3 ka (reaching 3.39E+12 per g TOC at 5.6 ka), but was not detected between 3.9 – 2.7 ka.

5. Discussion

Based on clear changes in TOC (Fig. 4~~2~~), colour and elemental signatures (Fig. 2 and 3~~-~~), we divided core 64PE418 into three widely acknowledged units, in line with previous studies (Jones & Gagnon, 1994; Arthur & Dean, 1998; Bahr et al., 2005). Unit III spans ~20 – 7.2 ka, covering the period where the Black Sea was a lacustrine environment, disconnected from the global ocean, and also the transition interval, where the basin moved towards a marine environment after the IMI over the Bosporus sill at ~9.6 ka (Aksu et al., 2002; Major et al.,

2006; Bahr et al., 2008; Ankindinova et al., 2019). Unit II (~7.2 – 2.6 ka) and Unit I (~2.6 ka - present) span the period where the Black Sea had become an anoxic brackish-to-marine environment. Diagenesis and preservation biases can affect lipid biomarker records, but since the records do not all mirror the oxygenation of the water column, and organic carbon contents remained relatively high, it is unlikely that diagenesis and preservation significantly influenced these records.

5.1. Oxic lacustrine phase (19.5 – 9.6 ka)

Throughout the last deglaciation and early Holocene (19.5 – 9.6 ka), TOC and TN levels are low, likely due to poor preservation of organic material, caused by the well-ventilated, oxygenated, freshwater environment that existed in the basin at this time (Schrader, 1979). Isorenieratene is not detected during this period, while elements that accumulate in sediment under anoxic conditions (i.e., Algeo and Li, 2020) also remained low (i.e., U, V, Mo; ~~see~~ Fig. 2~~. S2~~), which all points to a well-oxygenated environment. Freshwater/brackish conditions prevailed throughout this time, as shown by previous studies (Fig. S3~~5~~; Filipova-Marinova et al., 2013; Ion et al., 2022; Huang et al., 2022). Throughout this period, the abundance of Thaumarchaeota, indicated by crenarchaeol abundance, and anammox, indicated by the BHT-x ratio, remained relatively steady (Fig. 4). This stability is remarkable since the region experienced significant climatic changes which led to large variations in the surface water temperatures of the Black Sea, varying from ~10°C during the Bølling Allerød, ~7°C during the Younger Dryas and ~14°C by the Early Holocene (Ménot & Bard, 2012), as well as changes in the input of freshwater into the basin due regional precipitation variability and the melting of Eurasian icesheets and alpine glaciers (Bahr et al., 2005; 2006; 2008; Badertscher et al., 2011; Shumilovskikh et al., 2012; Filipova-Marinova et al., 2013; Ion et al., 2022). The subsurface stability is likely due to the stratification of the basin, where significant climatic shifts primarily impacted the surface waters, and the limited vertical mixing minimised the influence on subsurface waters, creating a stable environment for the subsurface nitrogen cycle. In contrast, changes in HG abundance and distribution suggest that surface-dwelling nitrogen-fixing cyanobacteria were sensitive to surface-water hydrological changes in the Black Sea over this period (Fig. 5~~3~~). The dominant HG structure varies between hexose C_{26} diol, hexose C_{28} diol and hexose C_{30} triol and after 11 ka, hexose C_{28} triol becomes present, which has been shown to be the major HG in members of the Rivulariaceae family (i.e., Calothix sp.) (Bauersachs et al., 2009). The warmer wetter conditions of the Early Holocene may have provided a trigger for this change in HG abundance and composition. Indeed, an increase in the abundance of the genus *Rivularia* was also noted in coastal regions of SW India during this period, coinciding with an increasingly warm and wet climate (Limaye et al., 2017). Another cause for this shift may have been related to changes in nutrient availability, with members of the Rivulariaceae family typically occurring in environments with highly variable phosphorus availability (Whitton & Mateo, 2012).

5.2. Transition phase (9.6 – 7.2 ka)

In line with existing research (Arthur & Dean, 1998; Bahr et al., 2006; 2008), the IMI occurred at ~9.6 ka, leading to a significant change in colour (Fig. S1~~2~~) and elemental composition of the sedimentary record (Fig. S2~~3~~), as

well as a substantial increase in abundance of HGs (Fig. 4). This increase does not coincide with higher TOC content, suggesting that enhanced preservation of HGs was not the cause. It is possible that these lipid biomarkers were transported fluvially to this site from lakes within the catchment basin of the Black Sea due to the warm/wet conditions at this time (Göktürk et al., 2011; Shumilovskikh et al., 2012; Filipova-Marinova et al., 2013). This, however, appears unlikely as our site is located a substantial distance from the mouths of major rivers (>230 km), and the BIT index remains low during this period (~0.08; pers. comms. B.Yang), indicating only a minor contribution of terrestrial organic matter at our site (Hopmans et al., 2004). Furthermore, as the proceeding period (7 – 5.6 ka) was also warm and wet (Göktürk et al., 2011; Shumilovskikh et al., 2012; Filipova-Marinova et al., 2013), we would expect the continuation of this peak if the HGs were being sourced from surrounding lacustrine environments. Instead, these high values decline abruptly after 6.6 ka.

It is therefore likely that the peak abundance in nitrogen-fixing cyanobacteria is related to warmer Black Sea surface temperatures during the early to mid-Holocene (Bahr et al., 2008) in combination with surface water stratification (Bahr et al., 2006). This stratification will have slowed the upward supply of fixed nitrogen, reducing nutrient availability in the surface waters, thereby promoting nitrogen-fixation by cyanobacteria (Hutchins & Fu, 2017). This stratification may have been driven in part by enhanced freshwater influx due to wetter conditions but may also have been triggered by the IMI through the Bosporus Strait at ~9.6 ka (Major et al., 2006; Bahr et al., 2008; Ankindinova et al., 2019). This IMI likely led to the gradual salinisation of the water column over this transition interval and intermittent build-up of anoxia in the water column. This, in turn, led to periods of higher preservation of organic matter compared to the preceding period, as indicated by the slight increase in TOC after 9.6 ka. The presence of isorenieratene after 9.4 ka indicates that anoxia reached the photic zone at intermittent periods during this transition interval, thereby providing sufficient conditions for the presence of the anoxygenic photoautotrophs, Chlorobiaceae. While the peak in nitrogen-fixing cyanobacteria occurs ~2 ka before anoxia intermittently entered the photic zone, the initial influx of dense saline water may have led to some reduction in vertical circulation, which reduced the amount of fixed nitrogen upwelled to the upper water column, leading to the presence of nitrogen-fixing cyanobacteria at 9.6 ka. This also coincides with a change in the distribution of HGs in our record between 9.7 – 6.9 ka where hexose C_{28} diol and hexose C_{30} triol increase in abundance and hexose C_{28} triol declines in relative abundance and is no longer present after 9.1 ka, coinciding with the presence of isorenieratene. These changes may reflect a shift in species composition, linked to the gradual salinisation and periodic anoxification of the water column after the IMI. The IMI at ~9.6 ka appears, however, to have had little impact on the abundances of anammox and Thaumarchaeota. This is possibly because basin-wide water column stratification and the permanent build-up of anoxia did not occur until later in the record, meaning that neither process instantaneously reacted to the IMI at ~9.6 ka.

5.3. Shift to anoxic brackish-to-marine mode of operation: a critical N-cycle threshold (~7.2 ka to present)

After 7.2 ka there was a substantial increase in TOC and TN and an abrupt shift in parts of the subsurface N-cycle. The latter is shown by an increase in the BHT-x ratio, indicating an intensification of anammox, which is coeval with a decrease in crenarchaeol, indicating that there was a decline in Thaumarchaeota-driven

nitrification. ~~-~~Studies have shown that by ~7.2 ka anoxia had built up in the water column, as indicated by changes in redox elements (Fig. S2 and Eckert et al., 2013; Wegwerth et al., 2018) and water column salinity had significantly increased (Fig. S~~35~~; Hiscott et al., 2007; Marret et al., 2009; Soulet et al., 2011; Filipova-Marinova et al., 2013), following the IMI from the Sea of Marmara at ~9.6 ka (Major et al., 2002; 2006; Bahr et al., 2005; 2008; Ankindinova et al., 2019). This is supported by the presence of isorenieratene in our record during this time, which indicates that anoxia penetrated the photic zone. This water column anoxia likely led to the enhanced preservation of TOC and TN and triggered a shift in the subsurface N-cycle, which crossed a threshold from an oxygenated lacustrine mode of operation to an anoxic brackish-to-marine mode of operation. The anoxic water column enabled anammox bacteria to expand their habitat from the anoxic sediments, where they likely were confined when the basin was an oxygenated freshwater environment, up into the suboxic/anoxic water column. This may therefore have commenced part of the modern-day N-cycle in the Black Sea where anammox activity occurs in the lower suboxic zone (~100 mbsl) where O_2 is (near) depleted and H_2S is absent (Jensen et al., 2008), with anammox bacteria consuming ammonium diffusing from the deep sea and utilising the nitrite produced by both Thaumarchaeota and ammonia-oxidising bacteria (AOB) (Kuypers et al., 2003; Lam et al., 2007). Consequently, it may be that the abundance of anammox bacteria increased as a result of the coupling to nitrite production by other microbes in the suboxic zone, whilst benefitting from ammonium diffusing upwards from the deep sea. The increased anammox after 7.1 ka likely indicates that more bioavailable nitrogen was lost from the system after the switch to the anoxic brackish-to-marine mode of operation. At the same time, Thaumarchaeota abundance declined, which may be in part due to the build-up of anoxia in the water column which reduced the niche of these aerobic microbes and the nitrification performed by them. Once these processes crossed a threshold from an oxygenated lacustrine mode of operation to an anoxic brackish-to-marine mode of operation, they appear to have remained steady for the remainder of the Holocene despite changes in the salinity of the basin (van der Meer et al., 2008; Mertens et al., 2012; Coolen et al., 2013) and significant changes in regional temperature and precipitation (Göktürk et al., 2011; Shumilovskikh et al., 2012; Filipova-Marinova et al., 2013). This shows that deoxygenation was the main driver of the observed change in annamox as well as archaeal nitrification and that they were not affected by hydrological changes mainly occurring at the surface. While our record shows centennial-scale changes in the N-cycle, we acknowledge that there may have also been rapid or short-term variations in N-cycle dynamics over this period that may not have been captured by the resolution of this record.

At 6.1 ka, the abundance of the HGs substantially declined, coinciding with an increase in $\delta^{15}N_{bulk}$, indicating a reduction in nitrogen fixation. This corresponds with the high-resolution record of Fulton et al., (2012) which also shows a decline in values at this time. As this decline in HG abundance and increase in $\delta^{15}N_{bulk}$ does not coincide with a reduction in TOC, it is unlikely that reduced preservation of HGs played a role here. As nitrogen-fixing cyanobacteria inhabit the upper surface layer, it is likely that this change is linked to the salinisation of the surface waters, with many studies demonstrating the disappearance of many freshwater mollusc, ostracod and dinoflagellate cyst species at this time, which were replaced by an increased abundance of euryhaline Mediterranean species (Hiscott et al., 2007; Marret et al., 2009; Filipova-Marinova et al., 2013; Ivanova et al.,

2015). At 6.1 ka, hexose C_{26} diol and hexose C_{28} diol are the only HGs present in the record, which may reflect the dominance of genera in the Nostocaceae family (i.e., Anabaena sp., Aphanizomenon sp., Nodularia sp., Nostoc sp.), as these members demonstrate a dominance of the hexose C_{26} diol and also contain varying amounts of hexose C_{28} diol (Gambacorta et al., 1999; Bauersachs et al., 2009). This distribution is similar to that of the Baltic Sea after ~7.2 ka when a series of weak intrusions of saline water led to the basin becoming fully brackish (Sollai et al., 2017). It is therefore possible that the peak in HGs in our Black Sea record between 9.6 – 6.9 ka represents a transition from the dominance of freshwater tolerant nitrogen-fixing cyanobacteria to more brackish species, with brackish species dominating the surface-waters after 6.6 ka. After 6.1 ka, $\delta^{15}N_{bulk}$ gradually decreases, indicating a rise in nitrogen fixation, ~~as~~ with this pattern also shown in previous ~~studies~~ records (Blumenberg et al., 2009; Fulton et al., 2012). While previous studies have shown riverine nitrogen to be a major source of fixed nitrogen in the modern Black Sea (McCarthy et al., 2007), due to the remoteness of our core site from the coast, our records are unlikely to have been significantly influenced by riverine input. It should be noted that a previous study (Fulton et al., 2012) ~~has~~ suggested, based on compound specific measurements of pyropheophytin, that sedimentary $\delta^{15}N$ in the Black Sea is primarily derived from eukaryotic algae rather than cyanobacteria which exhibits a different fractionation of nitrogen isotopes ~~(Fulton et al., 2012)~~. This means the use of $\delta 15N_{bulk}$ as a nitrogen fixation signal must be used with caution. HGs, however, are only derived from N-fixing cyanobacteria and are therefore an unambiguous biomarker of nitrogen fixation. Interestingly, at 4.3 ka pentose HGs are detected, coinciding with lowest $\delta^{15}N_{bulk}$, indicating the presence of marine nitrogen-fixing cyanobacteria found in symbiosis with marine diatoms. This indicates that the surface water salinity had reached a threshold which enabled these marine microbes to survive, with research indicating salinity reached ~17‰ during the deposition of Unit I (Ion et al., 2022) and freshwater/brackish species had disappeared by this time (Fig. S~~3~~5; Filipova-Marinova et al., 2013). Indeed, reported increases in the number of euryhaline species at this time also points to the increasing salinity of the surface waters (Marret et al., 2009; Bradley et al., 2012), which may be linked to warmer/drier conditions which reduced freshwater influx and/or enhanced evaporation (Göktürk et al., 2011). Between 3.9 – 2.7 ka, isorenieratene is not detected in the samples, reflecting the findings of previous studies (Sinninghe Damsté et al., 1993). It has been suggested that this resulted from the erosion of the chemocline (Sinninghe Damsté et al., 1993), while other research shows a short reoccurrence of freshwater/brackish species (Fig. S~~3~~5; Filipova-Marinova et al., 2013), which may indicate that enhanced freshwater input was responsible for lowering the chemocline below the photic zone. The disappearance of hexose HGs after 0.6 ka indicates that surface water salinities may more recently have become too high for the proliferation of brackish nitrogen-fixing cyanobacteria.

6. Conclusions

This study shows a relatively stable subsurface N-cycle in the Black Sea over the last deglaciation and Holocene with the exception of a critical threshold observed at 7.2 ka when the basin shifted from an oxygenated lacustrine environment to an anoxic brackish-to-marine basin. At this time, the loss of bioavailable nitrogen through anammox activity was enhanced and Thaumarchaeota-driven nitrification was reduced. Prior to, and after this transition, the subsurface N-cycle was remarkably stable despite various climatic and hydrological

changes that impacted the basin during the deglaciation and Holocene periods. Both the amount of nitrogen fixation by cyanobacteria and the composition of these microbes in the surface waters, however, appear to be much more dynamic and sensitive to hydrological changes over this period, responding in particular to salinity and temperature changes and stratification of the water column. Consequently, these records provide important insight into how future deoxygenation ~~and stratification~~ in marine environments may affect the microorganisms involved in the N-cycle, possibly ~~. While deoxygenation in marine environments may~~ leading to enhanced loss of bioavailable nitrogen by anammox, and reduced nitrification by Thaumarchaeota. Furthermore, in areas where enhanced ~~, enhanced stratification of the~~ water column stratification limits the supply of fixed nitrogen in the surface waters, localised ~~may lead to~~ enhanced cyanobacterial nitrogen fixation in the surface waters may occur. These changes may have associated feedbacks on nutrient cycling and carbon fixation, with implications for the future global carbon budget.

Data Availability

All data generated for this study are archived and publicly available via the Mendeley Data repository online at https://10.17632/4c9fg7jf5d.1 (Cutmore et al., 2024).

Acknowledgements

We thank the Chief Scientist Prof. Laura Villanueva as well as the captain and crew of the *R/V* Pelagia for the collection of core 64PE418. We would like to thank Jaap Sinninghe Damsté for useful discussions. For laboratory support we thank Anchelique Mets, Denise Dorhout and Monique Verweij. Research cruise 64PE418 was funded by the SIAM Gravitation Grant (024.002.002) from the Dutch Ministry of Education, Culture and Science (OCW). This study was funded by the Netherlands Earth System Science Centre (024.002.001) from the Dutch Ministry of Education, Culture and Science (OCW).

Author Contributions

Anna Cutmore: Conceptualization, Formal analysis, Investigation, Data Curation, Visualization, Writing - Original Draft, Writing - Review & Editing; Nicole Bale: Conceptualization, Methodology, Investigation, Supervision, Writing - Review & Editing; Rick Hennekam: Resources, Formal analysis, Investigation, Writing - Review & Editing; Darci Rush: Formal analysis, Writing - Review & Editing; Bingjie Yang: Formal analysis, Investigation, Writing - Review & Editing; Gert-Jan Reichart: Resources, Supervision, Writing - Review & Editing; Ellen C. Hopmans: Supervision; Stefan Schouten: Conceptualization, Supervision, Funding acquisition, Writing - Review & Editing

Competing interests: The authors declare that they have no conflict of interest.

References:

Aksu, A., Hiscott, R.N., Kaminski, M.A., Mudie, P.J., Gillespie, H., Abrajano, T and Yasar, D. 2002. Last glacial–Holocene paleoceanography of the Black Sea and Marmara Sea: stable isotopic, foraminiferal and coccolith evidence. *Marine Geology*, **190**, 119-149. doi.org/10.1016/S0025-3227(02)00345-6

Algeo, T.J and Li, C. 2020. Redox classification and calibration of redox thresholds in sedimentary systems. *Geochimica et Cosmochimica Acta*, **287**, 8-26. doi.org/10.1016/j.gca.2020.01.055

Ankindinova, O., Hiscott, R.N., Aksu, A.E and Grimes, V. 2019. High-resolution Sr-isotopic evolution of Black Sea water during the Holocene: Implications for reconnection with the global ocean. *Marine Geology*, **407**, 213-228. doi.org/10.1016/j.margeo.2018.11.004

Arthur & Dean, 1998. Organic-matter production and preservation and evolution of anoxia in the Holocene Black Sea. *Palaeoceanography & Palaeoclimatology,* **13**, 395-411. doi.org/10.1029/98PA01161

Badertscher, S., Fleitmann, D., Cheng, H., Edwards, R.L., Göktürk, O.M., Zumbühl, A., Leuenberger, M and Tüysüz, O. 2011. Pleistocene water intrusions from the Mediterranean and Caspian seas into the Black Sea. *Nature Geoscience*, **4**, 236–239. doi.org/10.1038/ngeo1106

Bale, N., Hopmans, E.C., Zell, C., Sobrinho, R.L., Kim, J.-H., Sinninghe Damsté, J.S., Villareal, T.A and Schouten, S. 2015. Long chain glycolipids with pentose head groups as biomarkers for marine endosymbiotic heterocystous cyanobacteria. *Organic Geochemistry*, **81**, 1-7. doi.org/10.1016/j.orggeochem.2015.01.004

Bale, N.J., Hennekam, R., Hopmans, E.C., Dorhout, D., Reichart, G.-J., van der Meer, M.T.J., Villareal, T.A., Sinninghe Damsté, J.S and Schouten, S. 2019. Biomarker evidence for nitrogen-fixing cyanobacterial blooms in a brackish surface layer in the Nile River plume during sapropel deposition. *Geology*, **47**, 1088–1092. doi.org/10.1130/G46682.1

Bale, N., Ding, S., Hopmans, E.C., Arts, M.G.I., Villanueva, L., Boschman, C., Haas, A.F., Schouten, S and Sinninghe Damsté, J.S. 2021. Lipidomics of Environmental Microbial Communities. I: Visualization of Component Distributions Using Untargeted Analysis of High-Resolution Mass Spectrometry Data. Frontiers in Microbiology, **12**, 1-15. doi.org/10.3389/fmicb.2021.659302

Bahr, A., Lamy, F., Arz, H., Kuhlmann, H and Wefer, G. 2005. Late glacial to Holocene climate and sedimentation history in the NW Black Sea. *Marine Geology*, **214**, 309-322. doi.org/10.1016/j.margeo.2004.11.013

Bahr, A., Arz, H., Lamy, F and Wefer, G. 2006. Late glacial to Holocene paleoenvironmental evolution of the Black Sea, reconstructed with stable oxygen isotope records obtained on ostracod shells. *Earth and Planetary Science Letters Volume*, **241**, 863-875. doi.org/10.1016/j.epsl.2005.10.036

494
495 Bahr, A., Lamy, F., Arz, H., Major, C., Kwiecien, O and Wefer, G. 2008. Abrupt changes of temperature and water
496 chemistry in the late Pleistocene and early Holocene Black Sea. *Geochemistry, Geophysics, Geosystems*, **9**, 1-16.
497 http://doi.org/10.1029/2007GC001683
498
499 Bauersachs, T., Compaoré, J., Hopmans, E.C., Stal, L.J., Schouten, S and Sinninghe Damsté, J. 2009. Distribution
500 of heterocyst glycolipids in cyanobacteria. *Phytochemistry*, **70**, 2034-2039.
501 doi.org/10.1016/j.phytochem.2009.08.014
502
503 Bauersachs, T., Speelman, E.N., Hopmans, E.C., Reichart, G.-J., Schouten, S and Sinninghe Damsté, J. 2010.
504 Fossilized glycolipids reveal past oceanic N2 fixation by heterocystous cyanobacteria. *Earth & Planetary Science*
505 *Letters*, **107**, 19190-19194. doi.org/10.1073/pnas.1007526107
506
507 Blaaw, M. 2010. Methods and code for 'classical' age-modelling of radiocarbon sequences. *Quaternary*
508 *Geochronology*, **5**, 512-518. doi.org/10.1016/j.quageo.2010.01.002
509
510 Blumenberg, M., Seifert, R., Kasten, S., Bahlmann, E and Michaelis, W. 2009. Euphotic zone bacterioplankton
511 sources major sedimentary bacteriohopanepolyols in the Holocene Black Sea. *Geochimica et Cosmochimica*
512 *Acta*, **73**, 750-766. doi.org/10.1016/j.gca.2008.11.005
513
514 Bopp, L., Resplandy, L., Orr, J.C., Doney, S.C., Dunne, J.P., Gehlen, M., Halloran, P., Heinze, C., Ilyina, T., Séférian,
515 R., Tjiputra, J and Vichi, M. 2013. Multiple stressors of ocean ecosystems in the 21st century: projections with
516 CMIP5 models. *Biogeosciences*, **10**, 6225–6245. doi.org/10.5194/bg-10-6225-2013
517
518 Bradley, L.R., Marret, F., Mudie, P. J., Aksu, A.E and Hiscott, R. N. 2012. Constraining Holocene sea-surface
519 conditions in the south-western Black Sea using dinoflagellate cysts. *Journal of Quaternary Science*, **27**, 835-843.
520 doi.org/10.1002/jqs.2580
521
522 Coolen, M.J.L., Orsib, W.D., Balkema, C., Quince, C., Harris, K., Sylva, S.P., Filipova-Marinova, M and Giosan, L.
523 2013. Evolution of the plankton paleome in the BlackSea from the Deglacial to Anthropocene. *PNAS*, **110**, 8609–
524 8614. doi.org/10.1073/pnas.1219283110
525
526 Czernik, J and Goslar, T. 2001. Preparation of Graphite Targets in the Gliwice Radiocarbon Laboratory for AMS
527 14C Dating. *Radiocarbon*, **43**, 283–291. doi.org/10.1017/S0033822200038121
528
529 Dalsgaard, T., Thamdrup, B., Farías, L and Revsbech, N.P. 2012. Anammox and denitrification in the oxygen
530 minimum zone of the eastern South Pacific. *Limnology & Oceanography*, **57**, 1331-1346.
531 doi.org/10.4319/lo.2012.57.5.1331

Eckert, S., Brumsack, H.-J., Severmann, S., Schnetger, B., März, C and Fröllje, H. 2013. Establishment of euxinic conditions in the Holocene Black. *Geology*, **41**, 431–434. doi.org/10.1130/G33826.1

Elling, F.J., Hemingway, J.D., Kharbush, J.J., Becker, K.W., Polik, C.A and Pearson, A. 2021. Linking diatom-diazotroph symbioses to nitrogen cycle perturbations and deep-water anoxia: Insights from Mediterranean sapropel events. *Earth and Planetary Science Letters*, **571**, 1-11. doi.org/10.1016/j.epsl.2021.117110

Falkowski, P.G., Barber, R.T and Smetacek, V. 1998.Biogeochemical controls and feedbacks on ocean primary production. *Science*, **281**, 200-206. doi.org/10.1126/science.281.5374.20

Filipova-Marinova, M., Pavlov, D., Coolen, M and Giosan, L. 2013. First high-resolution marinopalynological stratigraphy of Late Quaternary sediments from the central part of the Bulgarian Black Sea area. *Quaternary International*, **293**, 170-183. doi.org/10.1016/j.quaint.2012.05.002

Francis, C.A., Roberts, K.J., Beman, J.M., Santoro, A.E., Oakley, B.B. 2005. Ubiquity and diversity of ammonia-oxidizing archaea in water columns and sediments of the ocean. *Proceedings of the National Academy of Sciences of the USA*, **102**, 14683-14688. doi.org/10.1073/pnas.050662510

Fulton, J.M., Arthur, M.A and Freeman, K.H. 2012. Black Sea nitrogen cycling and the preservation of phytoplankton δ15N signals during the Holocene. *Global Biogeochemical Cycles*, **26**, 1-15. doi.org/10.1029/2011GB004196

Gambacorta, A., Trincone, A., Soriente, A and Sodano, G. 1999. Chemistry of glycolipids from the heterocysts of nitrogen-fixing cyanobacteria. *Phytochemistry*, **2**, 145–150.

Göktürk, O.M., Fleitmann, D., Badertscher, S., Cheng, H., Edwards, R.L., Leuenberger, M., Fankhauser, A., Tüysüz, O and Kramers, J. 2011. Climate on the southern Black Sea coast during the Holocene: implications from the Sofular Cave record. *Quaternary Science Reviews*, **30**, 2433-2445. doi.org/10.1016/j.quascirev.2011.05.007

Heaton, T.J., Köhler, P., Butzin, M., Bard, E., Reimer, R.W., Austin, W.E.N., Bronk Ramsey, C., Grootes, P.M., Hughen, K.A., Kromer, B., Reimer, P.J., Adkins, J., Burke, A., Cook, M.S., Olsen, J and Skinner, L.C. 2020. Marine20—The Marine Radiocarbon Age Calibration Curve (0–55,000 cal BP). *Radiocarbon*, **62**, 779–820. doi.org/10.1017/RDC.2020.68

Hennekam, R., van der Bolt, B., van Nes, E.H., de Lange, G.-J., Scheffer, M and Reichart, G.-J. 2020. Early-warning signals for marine anoxic events. *Geophysical Research Letters*, **47**, 1-9. doi.org/10.1029/2020GL089183

Hiscott, R.N., Aksu, A.E., Mudie, P.J., Marret, F., Abrajano, T., Kaminski, M.A., Evans, J., Çakiroğlu, A.İ., Yaşar, D. 2007. A gradual drowning of the southwestern Black Sea shelf: Evidence for a progressive rather than abrupt Holocene reconnection with the eastern Mediterranean Sea through the Marmara Sea Gateway. *Quaternary International*, **167–168**, 19-34. doi.org/10.1016/j.quaint.2006.11.007

Hopmans, E.C., Weijers, J.W.H., Schefuß, E., Herfort, L., Sinninghe Damsté, J.S and Schouten, S. 2004. A novel proxy for terrestrial organic matter in sediments based on branched and isoprenoid tetraether lipids. *Earth and Planetary Science Letters*, **224**, 107-116. doi.org/10.1016/j.epsl.2004.05.012

Hopmans, E.C., Smit, N.T., Schwartz-Narbonne, R., Sinninghe Damste, J.S and Rush, D. 2021. Analysis of non-derivatized bacteriohopanepolyols using UHPLC-HRMS reveals great structural diversity in environmental lipid assemblages. *Organic Geochemistry*, **160**, 1-17. doi.org/10.1016/j.orggeochem.2021.104285

Huang, Y., Zheng, Y., Heng, P., Giosan, L and Coolen, M.J.L. 2021. Black Sea paleosalinity evolution since the last deglaciation reconstructed from alkenone-inferred Isochrysidales diversity. *Earth and Planetary Science Letters*, **564**, 1-9. doi.org/10.1016/j.epsl.2021.116881

Ion, G., Briceag, A., Vasiliu, D., Lupaşcu, N and Melinte-Dobrinescu, M. 2022. A multiproxy reconstruction of the Late Pleistocene-Holocene paleoenvironment: New insights from the NW Black Sea. *Marine Geology*, **443**, 1-19. doi.org/10.1016/j.margeo.2021.106648

Ivanova, E.V., Murdmaa, I.O., Chepalyga, A.L., Cronin, T.M., Pasechnik, I.V., Levchenko, O.V., Howe, S.S., Manushkina, A.V and Platonova, E.A. 2007. Holocene sea-level oscillations and environmental changes on the Eastern Black Sea shelf. *Palaeogeography, Palaeoclimatology, Palaeoecology*, **246**, 228-259. doi.org/10.1016/j.palaeo.2006.09.014

Ivanova, E.V., Marret, F., Zenina, M.A., Murdmaa, I.O., Chepalyga, A.L., Bradley, L.R., Schornikov, E.I., Levchenko, O.V and Zyryanova, M.I. 2015. The Holocene Black Sea reconnection to the Mediterranean Sea: New insights from the northeastern Caucasian shelf. *Palaeogeography, Palaeoclimatology, Palaeoecology*, **427**, 41-61. doi.org/10.1016/j.palaeo.2015.03.027

Jaeschke, A., Hopmans, E. C., Wakeham, S. G., Schouten, S and Sinninghe Damsté, J.S. 2007. The presence of ladderane lipids in the oxygen minimum zone of the Arabian Sea indicates nitrogen loss through anammox. *Limnology and Oceanography*, **52**, 780–786. doi.org/10.4319/lo.2007.52.2.0780

606 Jensen, M.M., Kuypers, M.M.M., Lavik, G and Thamdrup, B. 2008. Rates and regulation of anaerobic ammonium
607 oxidation and denitrification in the Black Sea. *Limnology and Oceanography*, **53**, 23-36.
608 doi.org/10.4319/lo.2008.53.1.0023
609
610 Jones, G.A and Gagnon, A.R. 1994. Radiocarbon chronology of Black Sea sediments. *Deep-Sea Research 1*, **41**,
611 531-557. doi.org/10.1016/0967-0637(94)90094-9
612
613 Kalvelage, T., Lavik, G., Lam, P., Contreras, S., Arteaga, L., Löscher, C.R., Oschlies, A., Paulmier, A., Stramma, L
614 and Kuypers, M.M.M. 2013. Nitrogen cycling driven by organic matter export in the South Pacific oxygen
615 minimum zone. *Nature Geoscience*, **6**, 228-234. doi.org/10.1038/ngeo1739
616
617 Karner, M. B., DeLong, E. F., Karl, D. M. 2001. Archaeal dominance in the mesopelagic zone of the Pacific Ocean.
618 *Nature*, **409**, 507–510. doi.org/10.1038/35054051
619
620 Keeling, R.F., Körtzinger, A and Gruber, N. 2010. Ocean Deoxygenation in a Warming World. *Annual Review of*
621 *Marine Science*, **2**, 199-229. doi.org/10.1146/annurev.marine.010908.163855.
622
623 Knowles, R. 1982. Denitrification. *Microbiological Reviews*, **46**, 43-70. doi.org/10.1128/mr.46.1.43-70.1982.
624
625 Könneke, M., Bernhard, A.E., de la Torre, J.R., Walker, C.B., Waterbury, J.B and Stahl, D.A. 2005. Isolation of an
626 autotrophic ammonia-oxidizing marine archaeon. *Nature*, **437**, 543–546. doi.org/10.1038/nature03911
627
628 Koopmans, M.P., Köster, J., Van Kaam-Peters, H.M.E., Kenig, F., Schouten, S., Hartgers, W.A., de Leeuw, J.W and
629 Sinninghe Damsté, J.S. 1996. Diagenetic and catagenetic products of isorenieratene: Molecular indicators for
630 photic zone anoxia. *Geochimica et Cosmochimica Acta*, **60**, 4467-4496. doi.org/10.1016/S0146-6380(97)00025-
631 9
632
633 Kuenen, J.G and Robertson, L.A. 1988. Ecology of nitrification and denitrification. *In:* Cole, J.A and Ferguson, S.J
634 (eds.), The Nitrogen and Sulphur Cycles. Cambridge University Press, Cambridge, pp. 161-218.
635
636 Kusch, S., Wakeham, S.G and Sepúlveda, J. 2022. Bacteriohopanepolyols across the Black Sea redoxcline trace
637 diverse bacterial metabolisms. *Organic Geochemistry*, **172**, 1-18. doi.org/10.1016/j.orggeochem.2022.104462
638
639 Kuypers, M.M.M., Sliekers, A.O., Lavik, G., Schmid, M., Barker Jørgensen, B., Kuenen, J.G., Sinninghe Damsté,
640 J.S., Strous, M and Jetten, M.S.M. 2003. Anaerobic ammonium oxidation by anammox bacteria in the Black Sea.
641 Nature, 422, 608-611. doi.org/10.1038/nature01472
642

643 Kwiecien, O., Arz, H.W., Lamy, F., Wulf, S., Bahr, A., Röhl, U and Haug, G.H. 2008. Estimated Reservoir Ages of
644 the Black Sea Since the Last Glacial. *Radiocarbon*, 50, 99-118. doi.org/10.1017/S0033822200043393
645
646 Lam, P., Jensen, M.M., Lavik, G., McGinnis, D.F., Müller, B., Schubert, C.J., Amann, R., Thamdrup, B., and Kuypers,
647 M.M.M. 2007. Linking crenarchaeal and bacterial nitrification to anammox in the Black Sea. *PNAS*, **104**, 7104-
648 7109. doi.org/10.1073/pnas.061108110
649
650 Limaye, R.B., Padmalal, D and Kumaran, K.P.N. 2017. Cyanobacteria and testate amoeba as potential proxies for
651 Holocene hydrological changes and climate variability: Evidence from tropical coastal lowlands of SW India.
652 *Quaternary International*, **443**, 99-114. doi.org/10.1016/j.quaint.2016.09.044
653
654 Major, C., Ryan, W., Lericolais, G and Hajdas, I. 2002. Constraints on Black Sea outflow to the Sea of Marmara
655 during the last glacial–interglacial transition. Marine Geology, 190, 19-34. doi.org/10.1016/S0025-
656 3227(02)00340-7
657
658 Major, C., Goldstein, S., Ryan, W., Lericolais, G., Piotrowski, A.M and Hajdas, I. 2006. The co-evolution of Black
659 Sea level and composition through the last deglaciation and its paleoclimatic significance. *Quaternary Science*
660 *Reviews*, **25**, 2031-2047. doi.org/10.1016/j.quascirev.2006.01.032
661
662 Marret, F., Mudie, P., Aksu, A and Hiscott, R.N. 2009. A Holocene dinocyst record of a two-step transformation
663 of the Neoeuxinian brackish water lake into the Black Sea. *Quaternary International*, **197**, 72-86.
664 doi.org/10.1016/j.quaint.2007.01.010
665
666 McCarthy, J.J., Yilmaz, A., Coban-Yildiz, Y and Nevins, J.L. 2007. Nitrogen cycling in the offshore waters of the
667 Black Sea. Estuarine, Coastal and Shelf Science. 74, 493-514.
668
669 Ménot, G and Bard, E. 2012. A precise search for drastic temperature shifts of the past 40,000 years in
670 southeastern Europe. *Palaeoceanography*, **27**, 1-13. doi.org/10.1029/2012PA002291
671
672 Mertens, K.N., Bradley, L.R., Takano, Y., Mudie, P.R., Marret, F., Aksu, A.E., Hiscott, R.N., Verleye, T.J., Mousing,
673 E.A., Smyrnova, L.L., Bagheri, S., Mansor, M., Pospelova, V and Matsuoka, K. 2012. Quantitative estimation of
674 Holocene surface salinity variation in the Black Sea using dinoflagellate cyst process length. *Quaternary Science*
675 *Reviews*, **39**, 45-59. doi.org/10.1016/j.quascirev.2012.01.026
676
677 Murray, J.W., Jannasch, H. W., Honjo, S., Anderson, R. F., Reeburgh, W. S., Top, Z., Friederich, G. E., Codispoti, L.
678 A and Izdar, E. 1989. Unexpected changes in the oxic/anoxic interface in the Black Sea. *Nature*, **337**, 411-413.
679 doi.org/10.1038/338411a0
680

Murray, J.W., Codispoti, L.A and Friederich, G.E. 1995. Oxidation-reduction environments: the suboxic zone in the Black Sea. *In:* Huang C.P., O'Melia C.R., Morgan J.J. (Eds) Aquatic Chemistry: Interfacial and Interspecies Processes. ACS Advances in Chemistry Series. No. 224. pp. 157-176. doi.org/10.1021/ba-1995-0244.ch007

Naafs, B.D.A., Monteiro, F.M., Pearson, A., Higgins, M.B., Pancost, R.D and Ridgwell, A. 2019. Fundamentally different global marine nitrogen cycling in response to severe ocean deoxygenation. *Proceedings of the National Academy of Sciences*, **116**, 24979-24984. doi.org/10.1073/pnas.1905553116

Nicholas, W.A., Chivas, A.R., Murray-Wallace, C.V and Fink, D. 2011. Prompt transgression and gradual salinisation of the Black Sea during the early Holocene constrained by amino acid racemization and radiocarbon dating. *Quaternary Science Reviews*, **30**, 3769-3790. doi.org/10.1016/j.quascirev.2011.09.018

Özsoy, E and Ünlüata, Ü. 1997. Oceanography of the Black Sea: A review of some recent results. *Earth Science Reviews*, **42**, 231-272. doi.org/10.1016/S0012-8252(97)81859-4

Pérez Gallego, R., von Meijenfeldt, B., Bale, N.J., Sinninghe Damsté, J.S and Villanueva, L. 2025. Emergence and evolution of heterocyte glycolipid biosynthesis enabled specialized nitrogen fixation in cyanobacteria. Microbiology, 122. doi.org/10.1073/pnas.2413972122.

Piper, D.Z and Calvert, S.E. 2011. Holocene and late glacial palaeoceanography and palaeolimnology of the Black Sea: Changing sediment provenance and basin hydrography over the past 20,000 years. *Geochimica et Cosmochimica Acta*, **75**, 5597-5624. doi.org/10.1016/j.gca.2011.07.016

Ploug, H. 2008. Cyanobacterial surface blooms formed by Aphanizomenon sp. and Nodularia spumigena in the Baltic Sea: Small-scale fluxes, pH, and oxygen microenvironments. *Limnology & Oceanography*, **53**, 914-921. doi.org/10.4319/lo.2008.53.3.0914

Reimer, P.J., Austin, W.E.N., Bard, E., Bayliss, A., Blackwell, P.G., Bronk Ramsey, C., Butzin, M., Cheng, H., Edwards, R.L., Friedrich, N., Grootes, P.M., Guilderson, T.P., Hajdas, I., Heaton, T.J., Hogg, A.G., Hughen, K.A., Kromer, B., Manning, S.W., Muscheler, R., Palmer, J.G., Pearson, C., van der Plicht, J., Reimer, R.W., Richards, D.A., Scott, E.M., Southon, J.R., Turney, C.S.M., Wacker, L., Adolphi, F., Büntgen, U., Capano, M., Fahrni, S.M., Fogtmann-Schulz, A., Friedrich, R., Köhler, P., Kudsk, S., Miyake, F., Olsen, J., Reinig, F., Sakamoto, M., Sookdeo, A and Talamo, S. 2020. The IntCal20 Northern Hemisphere Radiocarbon Age Calibration Curve (0–55 cal kBP). *Radiocarbon*, **62**, 725–757. doi.org/10.1017/RDC.2020.41

Rush, D., Sinninghe Damsté, J.S., Poulton, S.W., Thamdrup, B., Garside, A.L., Acuña González, J., Schouten, S., Jetten, M.S.M and Talbot, H.M. 2014. Anaerobic ammonium-oxidising bacteria: A biological source of the

718 bacteriohopanetetrol stereoisomer in marine sediments. *Geochimica et Cosmochimica Acta*, **140**, 50-64.
719 doi.org/10.1016/j.gca.2014.05.014
720
721 Rush, D and Sinninghe Damsté, J.S. 2017. Lipids as paleomarkers to constrain the marine nitrogen cycle.
722 *Environmental Microbiology*, **19**, 2119-2132. doi.org/10.1111/1462-2920.13682
723
724 Schouten, S., Hopmans, E.C and Sinninghe Damsté, J.S. 2013. The organic geochemistry of glycerol dialkyl
725 glycerol tetraether lipids: A review. *Organic Geochemistry*, **54**, 19-61.
726 doi.org/10.1016/j.orggeochem.2012.09.006
727
728 Schrader, H.-J. 1979. Quaternary Paleoclimatology of the Black Sea basin. *Sedimentary Geology*, **23**, 165-180.
729 doi.org/10.1016/0037-0738(79)90013-7
730
731 Schwartz-Narbonne, N., Schaeffer, P., Hopmans, E.C., Schenesse, M., Charlton, E.A., Jones, D.M., Sinninghe
732 Damsté, J.S., Farhan, M., Haque, U., Jetten, M.S.M., Lengger, S.K., Murrell, J.C., Normand, P., Nuijten, G.H.L.,
733 Talbot, H.M and Rush, D. 2020. A unique bacteriohopanetetrol stereoisomer of marine anammox. *Organic*
734 *Geochemistry*, **143**, 1-10. doi.org/10.1016/j.orggeochem.2020.103994
735
736 Shumilovskikh, L.S., Tarasov, P., Arz, H.W., Fleitmann, D., Marret, F., Nowaczyk, N., Plessen, B., Schlütz, F and
737 Behling, H., 2012. Vegetation and environmental dynamics in the southern Black Sea region since 18 kyr BP
738 derived from the marine core 22-GC3. *Palaeogeography, Palaeoclimatology, Palaeoecology*, **337–338**, 177-193.
739 doi.org/10.1016/j.palaeo.2012.04.015
740
741 Sinninghe Damste, J.S., Wakeham, S.G., Kohnen, M.E.L., Hayes, J.M., de Leeuw, J.W. 1993. A 6,000–year
742 sedimentary molecular record of chemocline excursions in the Black Sea. *Nature*, **362**, 827–829.
743 doi.org/10.1038/362827a0
744
745 Sinninghe Damsté, J.S., Schouten, S., Hopmans, E.C., van Duin, A.C.T and Geenevasen, A.J.A. 2002. Crenarchaeol.
746 *Journal of Lipid Research*, **43**, 1641-1651.
747
748 Sollai, M., Hopmans, E.C., Bale, N.J., Mets, A., Warden, L., Moros, M and Sinninghe Damsté, J.S. 2017. The
749 Holocene sedimentary record of cyanobacterial glycolipids in the Baltic Sea: an evaluation of their application
750 as tracers of past nitrogen fixation. *Biogeosciences*, **14**, 5789–5804. doi.org/10.5194/bg-14-5789-2017
751
752 Soulet, G., Ménot, G., Lericolais, G and Bard, E. 2011. A revised calendar age for the last reconnection of the
753 Black Sea to the global ocean. *Quaternary Science Reviews*, **30**, 1019-1026.
754 doi.org/10.1016/j.quascirev.2011.03.001
755

Stuiver, M and Polach, H.A. 1977. Discussion Reporting of 14C Data. *Radiocarbon*, **19**, 35-363. doi.org/10.1017/S0033822200003672

van de Graaf, A.A., de Bruijn, P., Robertson, L.A., Jetten, M.S.M and Kuenen, J.G. 1997. Metabolic pathway of anaerobic ammonium oxidation on the basis of 15N studies in a fluidized bed reactor. *Microbiology*, **143**, 2415–2421. doi.org/10.1099/00221287-143-7-2415

van der Meer, M.J.M., Sangiorgi, F., Baas, M., Brinkhuis, H., Sinninghe Damsté, J.S and Schouten, S. 2008. Molecular isotopic and dinoflagellate evidence for Late Holocene freshening of the Black Sea. *Earth and Planetary Science Letters*, **267**, 426-434. doi.org/10.1016/j.epsl.2007.12.001

van Kemenade, Z.R., Cutmore, A., Hennekam, R., Hopmans, E.C., van der Meer, M.T.J., Mojtahid, M., Jorissen, F.J., Bale, N.J., Reichart, G.-J., Sinninghe Damsté, J.S and Rush, D. 2023. Marine nitrogen cycling dynamics under altering redox conditions: insights from deposition of sapropels S1 and the ambiguous S2 in the Eastern Mediterranean Sea. *Geochimica et Cosmochimica Acta*, **354**. doi.org/10.1016/j.gca.2023.06.018

Verleye, T.J., Mertens, K.N., Louwye, S and Arz, H.W. 2009. Holocene salinity changes in the southwestern black sea: A reconstruction based on dinoflagellate cysts. *Palynology*, **33**, 77-100.

Villareal, T.A. 1992. Marine Nitrogen-Fixing Diatom-Cyanobacteria Symbioses. *In:* Carpenter, E.J., Capone, D.G and Rueter, J. G (eds.), Marine Pelagic Cyanobacteria: Trichodesmium and other Diazotrophs. Springer:Dordrecht, pp. 163-175.

Wegwerth, A., Eckert, S., Dellwig, O., Schnetger, B., Severmann, S., Weyer, S., Brüske, A., Kaiser, J., Köster, J., Arz, H.W and Brumsack, H.-J. 2018. Redox evolution during Eemian and Holocene sapropel formation in the Black Sea. *Palaeogeography, Palaeoclimatology, Palaeoecology*, **489**, 249-260.

Whitton, B.A and Mateo, P. 2012. Rivulariaceae. In: Whitton, B.A (ed.), Ecology of Cyanobacteria II. Springer:Dordrecht, pp. 561–591. doi.org/10.1007/978-94-007-3855-3_22

Wörmer, L., Cires, S., Velazquez, D., Quesada, A and Hinrichs, K.-U. 2012. Cyanobacterial heterocyst glycolipids in cultures and environmental samples: Diversity and biomarker potential. *Limnology & Oceanography*, **57**, 1775-1788. doi.org/10.4319/lo.2012.57.6.1775

Wuchter, C., Abbas, B., Coolen, M.J.L., Herfort, L., van Bleijswijk, J., Timmers, P., Strous, M., Teira, E., Herndl, G.J., Middelburg, J.J., Schouten, S and Sinninghe Damsté, J.S. 2006. Archaeal nitrification in the ocean. *PNAS*, **103**, 12317-12322. doi.org/10.1073/pnas.0600756103

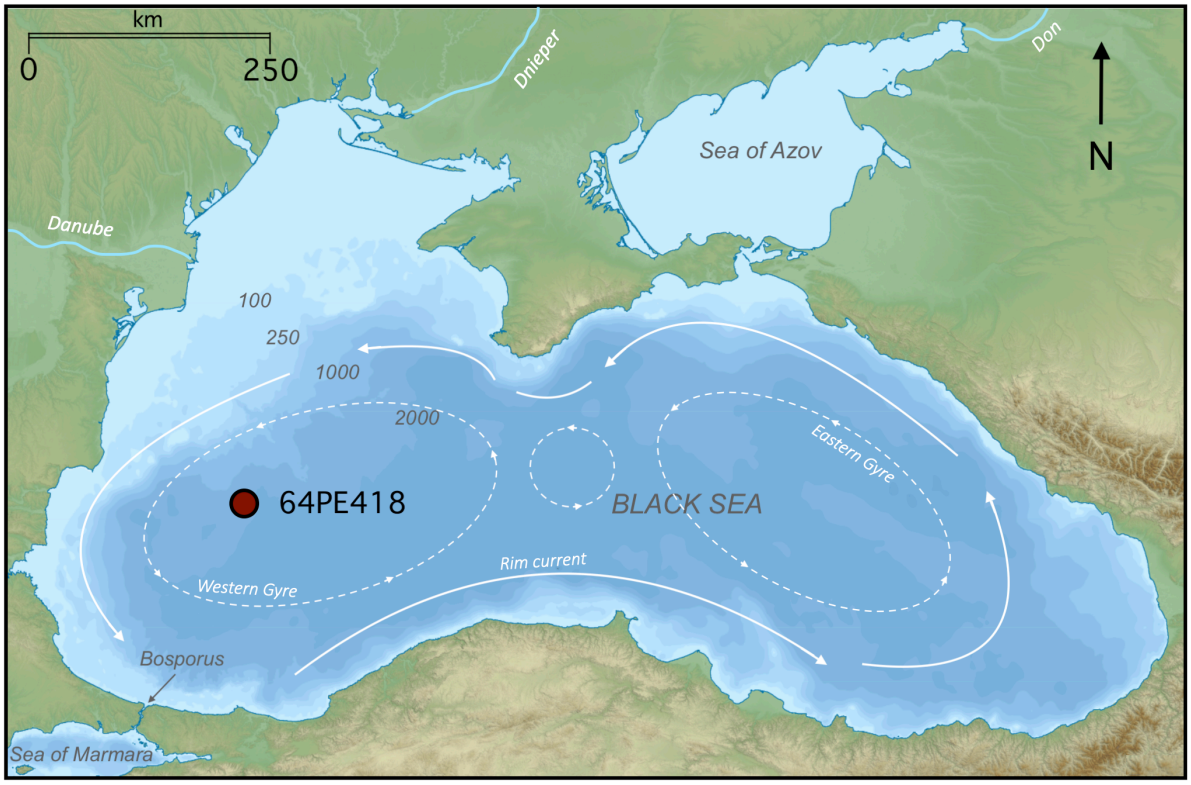

Figure 1: Map of the Black Sea basin, showing the major surface circulation, depth contours (mbsl) and location of core 64PE418. (Adapted from: Giorgi Balakhadze, English Wikipedia, 2016).

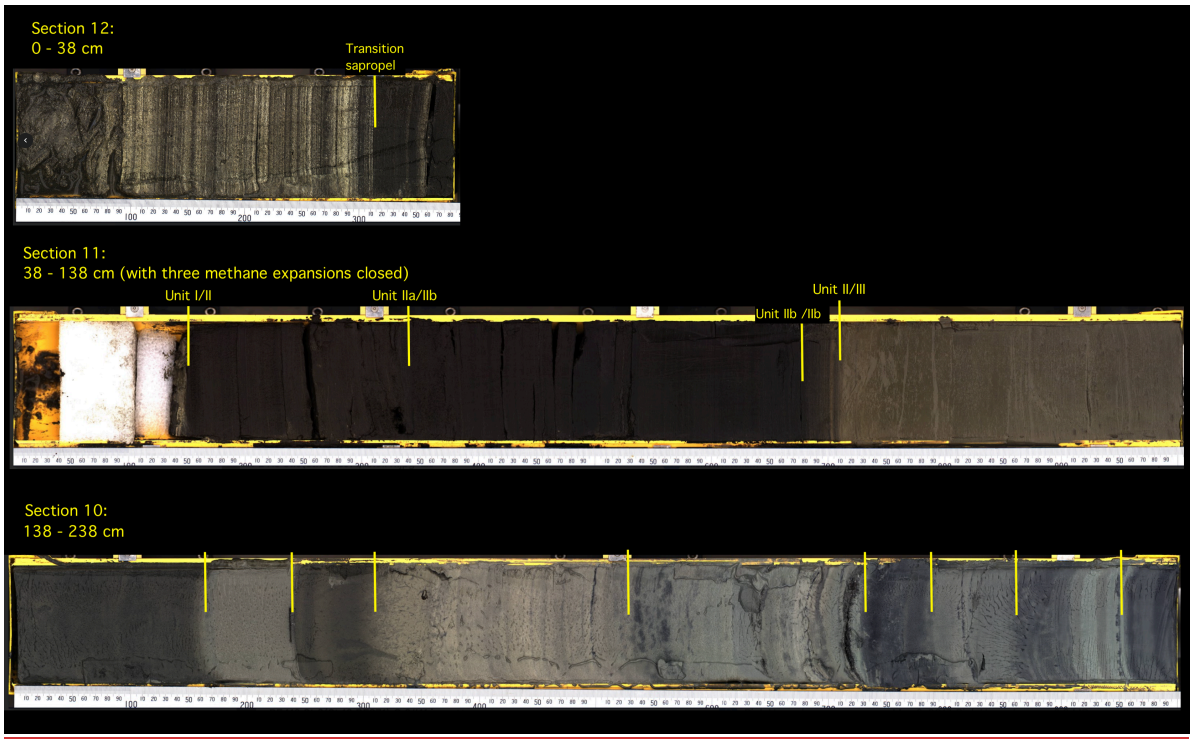

Figure 2: Scan of core 64PE418 showing colour changes and the depth of unit boundaries. Unit boundaries are defined according to Arthur & Dean (1998) and have been identified by colour changes and XRF-core-scan changes in Ti and Ca (Fig. S1).

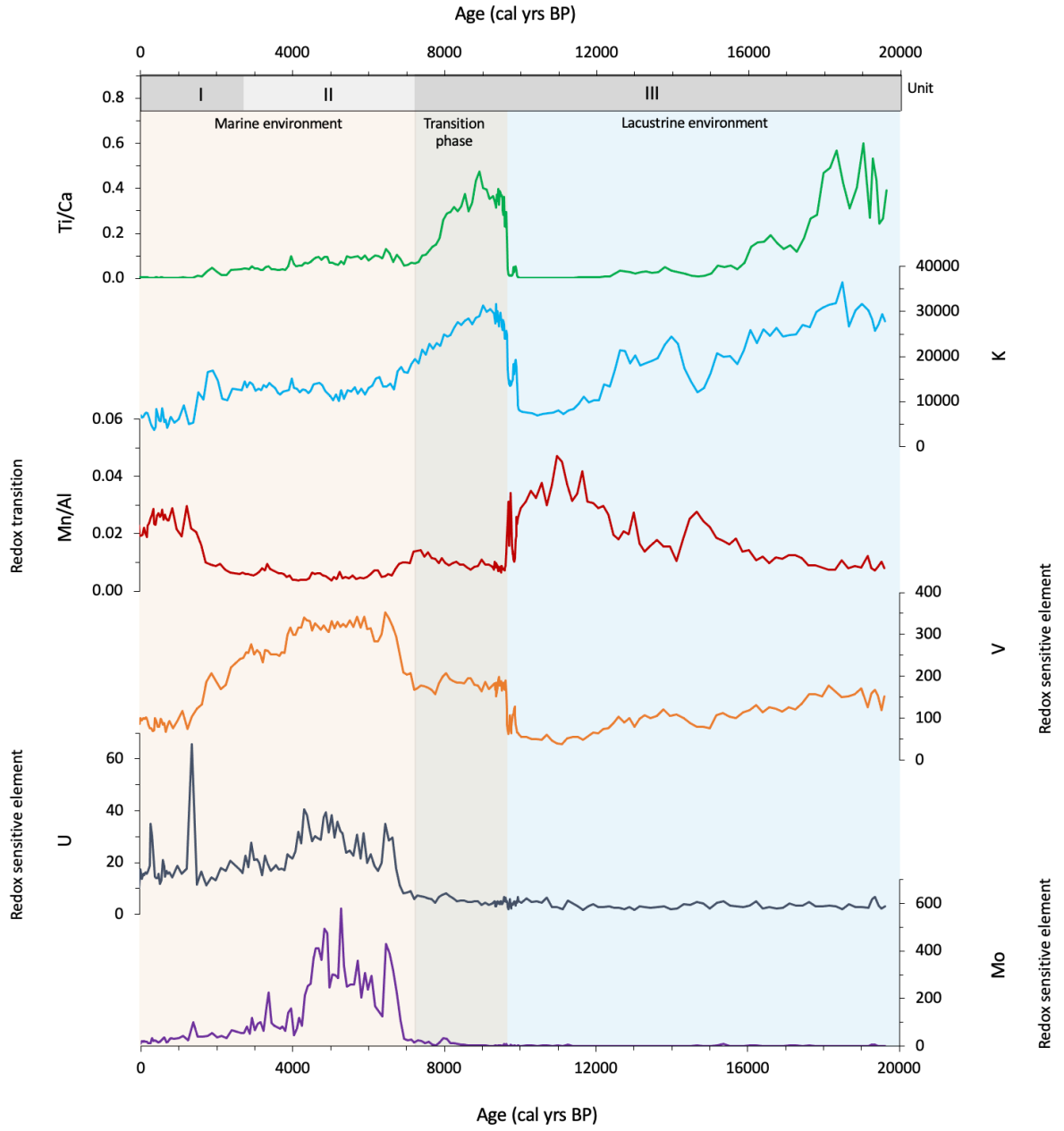

Figure 3: Changes over the last 19.6 ka in the elemental content of core 64PE418, as measured through calibrated XRF-core-scanning (ppm) using the methods described in Hennekam et al. (2020).

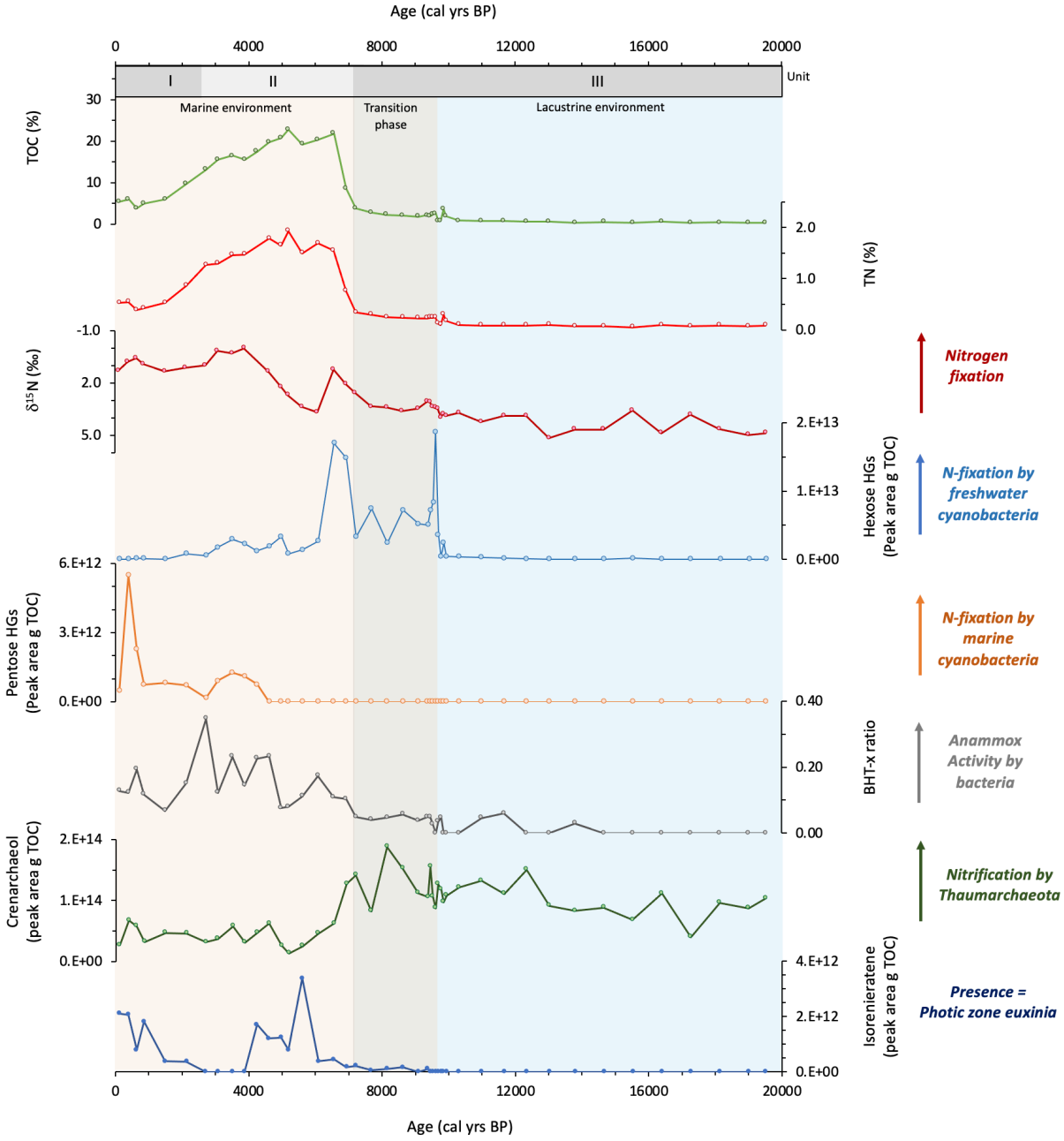

Figure 4: Geochemical records from Black Sea core 64PE418 of: a) TOC (%); b) TN (%); c) $\delta^{15}N_{bulk}$ (‰); d) hexose HGs (peak area per g TOC); e) pentose HGs (peak area per g TOC); f) BHT-x ratio; g) crenarchaeol (peak area per g TOC); h) isorenieratene (peak area per g TOC).

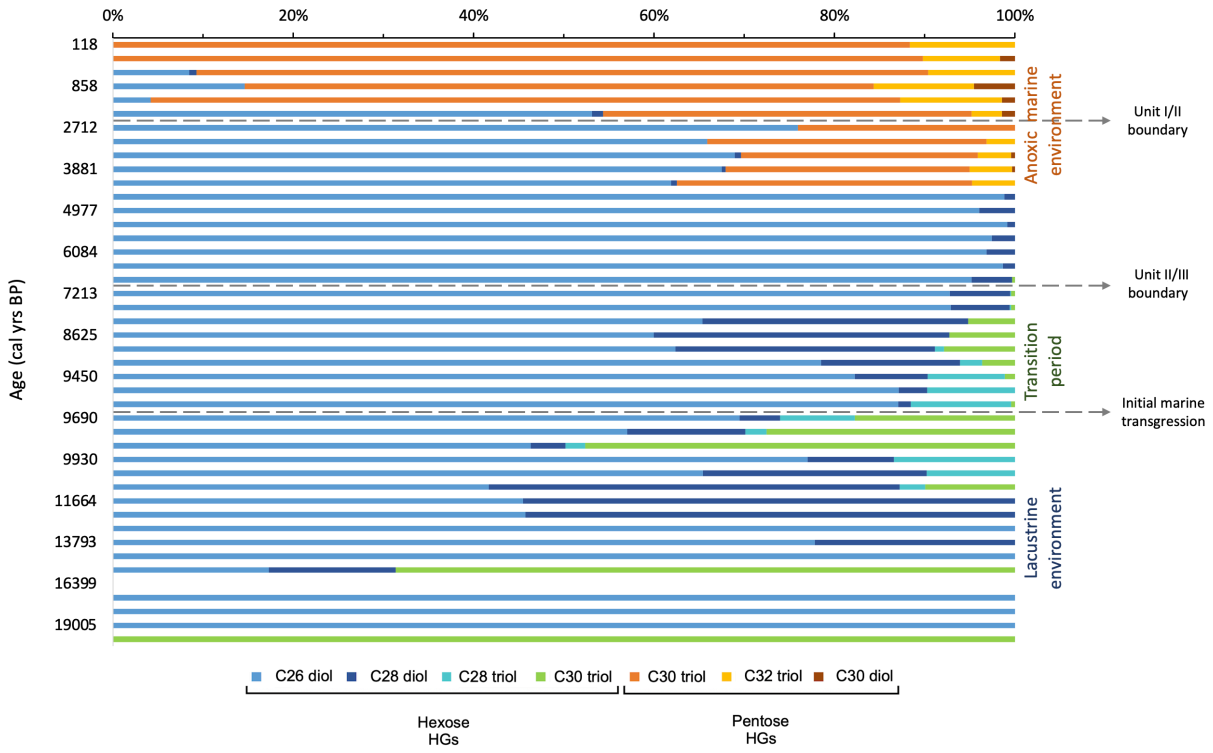

Figure 5: Changes over time in relative abundance of hexose and pentose HGs present in Black Sea core 64PE418

~~**Table 1:** Outline of the seven ^{14}C dates used in the production of the age-model for core 64PE418 and their calibrated ages. The ^{14}C and calibrated age of 142.5 cm is shown but was excluded from the age-depth model due to an age reversal.~~

~~Core~~	~~Depth (cm)~~	~~Material~~	~~Radiocarbon age (^{14}C yr BP)~~	~~± 1σ~~	~~Calendar age (cal yr BP)~~	~~± 2σ~~
~~64PE418[a]~~	~~24.5~~	~~TOC~~	~~2010~~	~~30~~	~~435[c,e]~~	~~115~~
~~KNR134-08-BC17[b]~~	~~39.0~~	~~TOC~~	~~3640~~	~~70~~	~~2145[c,e]~~	~~205~~
~~64PE418[a]~~	~~76.5~~	~~TOC~~	~~5795~~	~~35~~	~~4870[c,e]~~	~~170~~
~~64PE418[a]~~	~~118.5~~	~~TOC~~	~~9110~~	~~50~~	~~9328[d,f]~~	~~128~~
~~***64PE418[a]***~~	~~***142.5***~~	~~***TOC***~~	~~***11650***~~	~~***60***~~	~~***12720[d,g]***~~	~~***50***~~
~~64PE418[a]~~	~~158.5~~	~~TOC~~	~~9670~~	~~50~~	~~9975[d,f]~~	~~205~~
~~64PE418[a]~~	~~183.5~~	~~TOC~~	~~12380~~	~~70~~	~~13358[d,g]~~	~~123~~
~~64PE418[a]~~	~~217.5~~	~~TOC~~	~~17420~~	~~110~~	~~19270[d,h]~~	~~250~~

~~*a 14C dates from this study*~~

~~*b 14C dates from Jones & Gagnon, 1994*~~

~~*c Calibrated with the Marine20 curve (Heaton et al., 2020)*~~

~~*d Calibrated with the IntCal20 curve (Reimer et al., 2020)*~~

~~*e R-age of 600 years applied (Kwiecien et al., 2008)*~~

~~*f R-age of 800 years applied (Kwiecien et al., 2008)*~~

~~*g R-age of 900 years applied (Kwiecien et al., 2008)*~~

~~*h R-age of 1450 years applied (Kwiecien et al., 2008)*~~